



You have downloaded a document from
RE-BUŚ
repository of the **University of Silesia in Katowice**

Title: Fault Dimensions and Displacements in Mining Area: Northern Part of the Upper Silesian Coal Basin

Author: Lesław Teper

Citation style: Teper Lesław. (1996). Fault Dimensions and Displacements in Mining Area: Northern Part of the Upper Silesian Coal Basin. W: A. Idziak (red.), "Tectonophysics of mining areas" (S. 41-56). Katowice : Uniwersytet Śląski



Uznanie autorstwa - Użycie niekomercyjne - Bez utworów zależnych Polska - Licencja ta zezwala na rozpowszechnianie, przedstawianie i wykonywanie utworu jedynie w celach niekomercyjnych oraz pod warunkiem zachowania go w oryginalnej postaci (nie tworzenia utworów zależnych).



UNIWERSYTET ŚLĄSKI
W KATOWICACH



Biblioteka
Uniwersytetu Śląskiego



Ministerstwo Nauki
i Szkolnictwa Wyższego

LESŁAW TEPER*

Fault Dimensions and Displacements in Mining Area: Northern Part of the Upper Silesian Coal Basin

Abstract

Fault network of northern part of the Upper Silesian Coal Basin (the USCB) was mapped with regards to structures having more than 1 m of vertical throw that were surveyed in mine driving roadways and worked panels of coal. The map was digitized on SUN workstation using ZYCOR software. Parameters of size and geometry catalogued while digitizing for each item considered were, as follows:

- 1) local Cartesian coordinates of the fault terminations (Sucha Góra grid),
- 2) attachment to a proper azimuthal set defined by vectorial analysis,
- 3) order (rank) of the structure interpreted by means of structural analysis,
- 4) maximum throw,
- 5) angle of dip of the fault surface.

Original programs were created for data selection. They enabled sampling populations with optionally established limits of separate fault features listed above. One can figure out and depict on graphs relationships between the parameters employing programs made for analysis of these particular data sets.

Relationship between width of a fault and its maximum throw is ruled by power function with exponent between 1.5 and 2.0. The result is nearest to those presented in the last papers by the team of the Fault Analysis Group from the University of Liverpool (Gillespie et al., 1992). Distribution of dimension in the fault population is illustrated on log-log graphs by curve which may be estimated by a straight line whose slope is equal -2.3 roughly.

Obtained results are comparable with those concerning another regions and/or groups of faults from variety of geological environments provided by other scientists. Their position in combined dataset is useful for adjusting existing models and interpretations, especially they help with stating more precisely formulae that express scaling laws governing the relationships studied.

The displacement/dimension relationship determined precisely implies more accurate description of fault growth over geological time. Furthermore, this relationship gives a possibility to calculate total

* Lesław Teper – Wydział Nauk o Ziemi, Uniwersytet Śląski, 41-200 Sosnowiec, ul. Będzińska 60.

brittle strain for this deformed rock-complex. Therefore the study on faults displacement and dimension, as well as essential follow-ups are of such importance for the USCB area.

Introduction

Northern part of the Upper Silesian Coal Basin (the USCB) is a testing area for an examination of relationship between mining tremors occurrence and a rock-mass structure. The research has been carried out by a team of Department of Applied Geology of the Silesian University at Sosnowiec with support of Polish Government. At the first stage fault network of the rectangular area (28×16 km) in

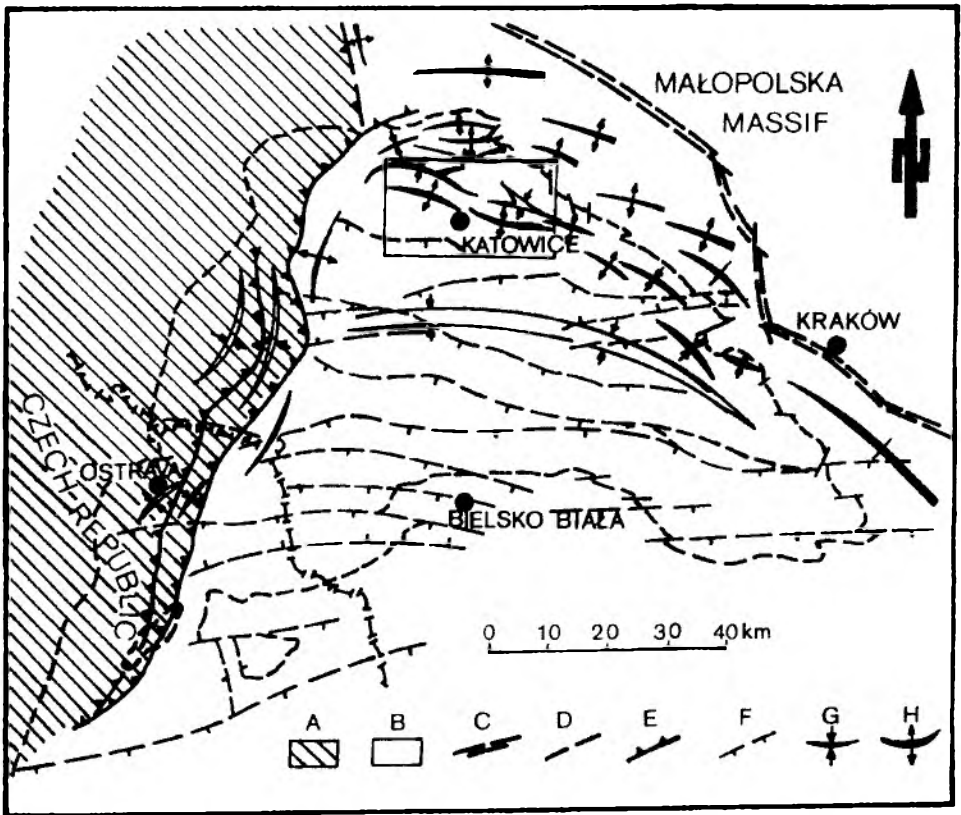


Fig. 1. Study area on the background of tectonic simplified map of the Upper Silesian Coal Basin after J. Jureczka & A. Kotas (1995)

A – zone of fold tectonics, B – zone of fault-block tectonics, C – the Cracow deep-seated fault zone, D – boundary of the USCB, E – overthrusts, F – main faults formed or modified during Alpine tectogenesis, G – synclines, H – anticlines. Location of Fig. 2 (the study area) is also shown as a frame

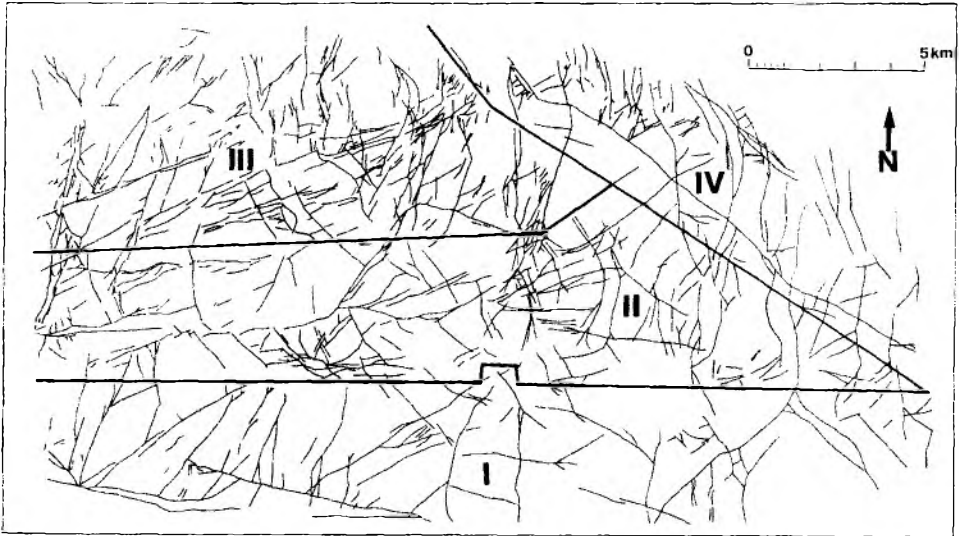


Fig. 2. Generalised fault map (modified after e.g. Goszcz, 1980; Goszcz et al., 1983) of the northern part of the USC B (cf., Fig. 1)

I – the Kłodnicki fault system, II – the Saara fault system, III – Fault sets of the Bytom syncline, IV – the Będziński fault system

the region studied (Fig. 1) was mapped for the project purpose. The map (Fig. 2) was made as a sum of archival records and current data concerning faulting details which were derived from original large-scale plans produced by mining surveyors for coal seam surfaces (e.g. Goszcz et al., 1983). All features having vertical throw down to 1 m which were measured directly in driving roadways and face headings were shown on the map. There are extensive workings in many seams over a vertical range of up to 1000 m. Occasionally, shaft and borehole records provide point data between seams. It yielded an information about 3-D geometry of faults and enabled fault traces to be projected on sea level in their maximum dimensions recorded directly.

Size Parameters of an Ideal Single Fault

Fault geometry is usually represented either by fault traces on maps and seam plans, or by cross-sections. There are, however, some aspects which are best visible on strike-projections introduced by scientists from the University of Liverpool (i.e., Watterson, 1986; Walsh, Watterson, 1988, 1990; Gillespie et al., 1992). Strike-projections of tectonic faults for which there are sufficient dis-

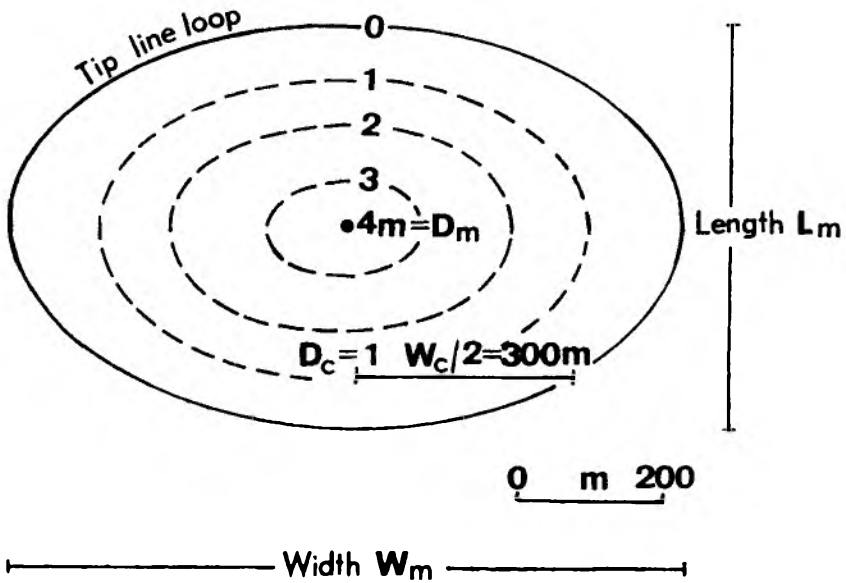


Fig. 3. Schematic displacement contour strike projection of an idealised fault surface (modified after Walsh & Watterson, 1988) bounded by a zero displacement contour with maximum displacement D_m , in centre

Displacement, D_c , is the maximum displacement along a chord of half-width, $W_c/2$. Width, W_m , and length, L_m , of the fault are also shown

placement readings show that displacement (D) varies systematically over a fault surface. In the case of an ideal fault the maximum displacement (D_m) lies in the centre of the fault surface and the tip-line loop, where displacement is reduced to zero, approximates to an ellipse (Rippon, 1985) with an axial ratio of about 2 (Walsh, Watterson, 1990). Figure 3 shows the geometry of the ideal normal fault which does not intersect a free surface. The fault width (W_m) is defined as the maximum dimension of the surface in a direction normal to the slip direction and the fault length (L_m) is the maximum dimension parallel to the slip direction. These dimensions can be determined only in cases where the fault surface is mapped in three dimensions. Fault traces derived from maps are chords on the fault surface with the chord lengths designated (after Gillespie et al., 1992) W_c in the case of normal and reverse faults, and L_c in the instance of strike-slip faults. In such cases the maximum displacement on a mapped fault trace (D_c) may be the only value obtainable. Thus, when derived from a map trace measurement, the dimension and displacement of fault are usually underestimated. W , L and D without subscripts refer to data for either maximum or chord dimensions/displacements where distinction is not possible.

Data Preparation

The fault map of northern part of the USCB was digitized (Fig. 4) on SUN workstation using ZYCOR software which is very helpful in solving geological, cartographical and geophysical problems. Parameters of size and geometry catalogued while digitizing for each item considered were, as follows:

- 1) local Cartesian x and y coordinates of the fault terminations (Sucha Góra grid),
- 2) attachment to a proper azimuthal set defined by vectorial analysis of fault position done for whole population considered,
- 3) order (rank) of the structure interpreted by means of structural analysis,

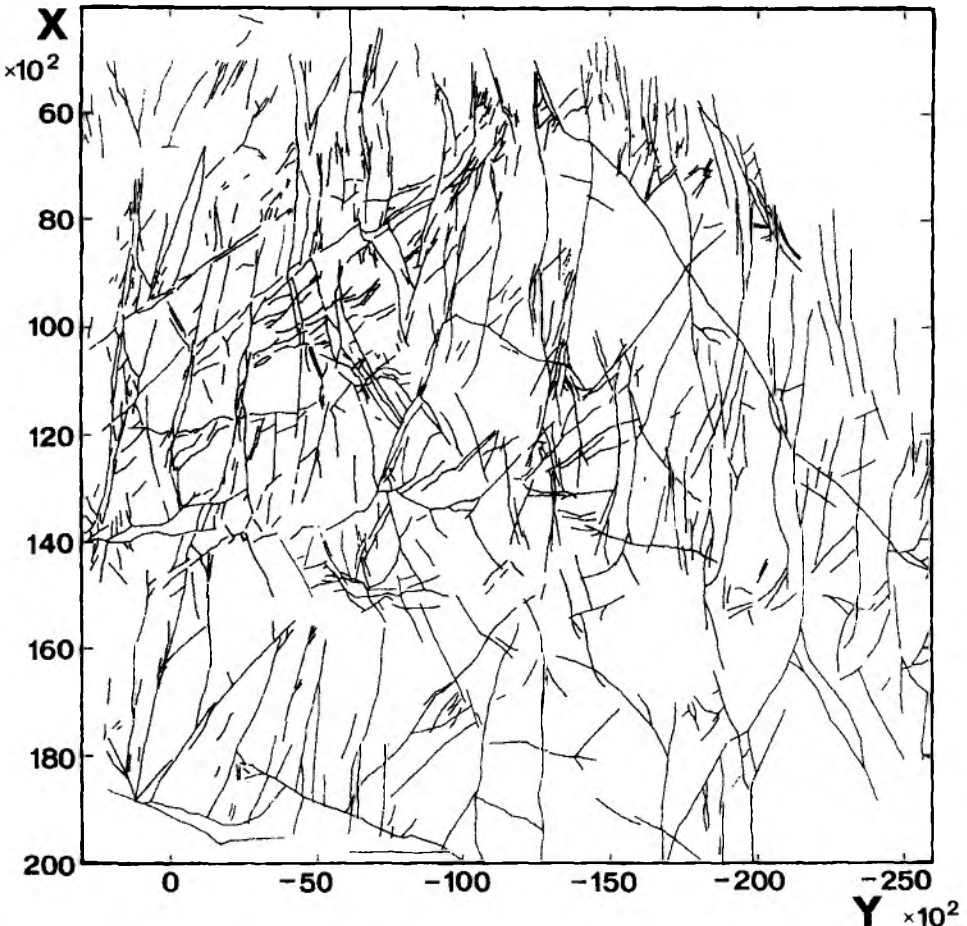


Fig. 4. Digitized fault map of the study area (cf., Fig. 2)

Version obtained using PC and a plotter

- 4) maximum throw,
- 5) angle of dip of the fault surface.

974 features were digitized in this manner. In the cases when strike azimuth or dip angle changed along fault trace, the attributes of size and geometry were put down to fault segments isolated according to sections with stable values of those parameters.

Data set was extracted and accommodated to working on PC. Original programs were created for data selection. They enabled sampling populations with optionally established limits of separate fault attributes listed above (Fig. 5). In this meaning one can, for example, create classes taking into account fault distribution within the specific territorial bounds and/or IIRd rank features only and/or members of submeridional set and/or faults having throws of over or below certain value. Each class chosen may be presented either as a data file, or as a graph (map) on PC monitor, which may be copied using printer or plotter.

One can also figure out and depict on graphs relationships between the parameters employing programs made for analysis of these particular data sets. Fault size frequency distribution and the relationship between fault width and displace-

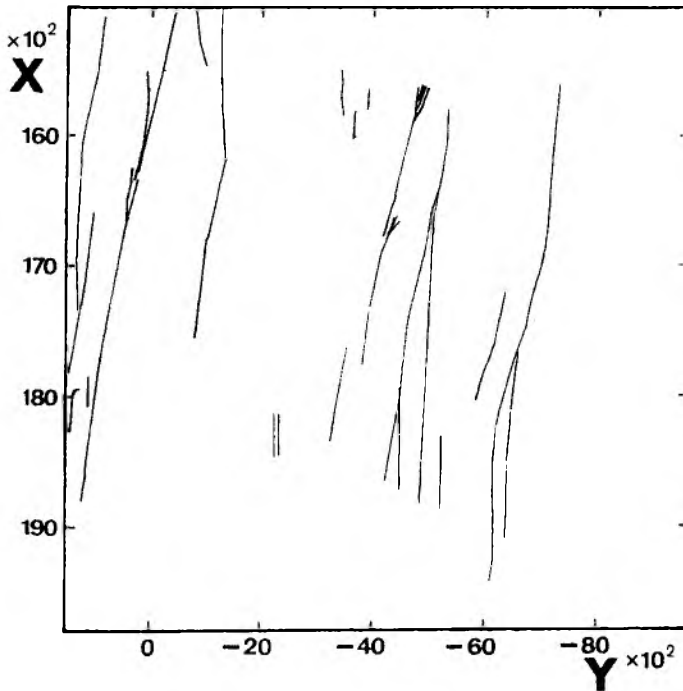


Fig. 5. Fault population sample chosen with regard to both territorial extent (note x , y local coordinates) and an affiliation to the azimuthal class (submeridional set)

Version obtained using PC and a plotter. Zoom-in reveals branching splays occurring in the area

ment are the subject of the next two chapters. The analysis was made either for the entire population, and for small sectors which were distinguished in respect of level of mining works or number of feature records. The latter part of analysis enables to find possible differences in the relationship profiles obtained for regions of poor and reliable documentation.

Results and their Discussion

Relationship between Dimension and Displacement of Fault

The relationship between dimension and displacement of faults is shown as logarithmic plots of width, W_m , against maximum displacement, D_m (Figs 6, 7). Analysis showed that D versus W scaling relationship is non-linear and that rather a power-law relationship exists, exponent values of which range from 1.0 to 2.0 roughly. The value close to 2.0 is obtainable when the entire population or large region are analysed (Fig. 6). Smaller sets of features appear to obey power-law with an exponent value not exceeding 1.5, sometimes close to 1.0 (Fig. 7).

Many datasets were analysed so far using the same method (e.g. Mac Millan, 1975; Elliott, 1976; Ranalli, 1977; Muraoka, Kamata, 1983; Walsh, Watterson, 1988; Scholz, Cowie, 1990; Cowie, Scholz, 1992; Gillespie et al., 1992). All the same, it needs an emphasis that among numerous published datasets the only one, that of J. J. Walsh & J. Watterson (1988) comprises more than 500 individual faults (552 items) resembling the Upper Silesian set in respect of both number and provenience. It provides data from British coalfield (Derbyshire and Yorkshire). R. A. Mac Millan (1975) and G. Ranalli (1977) collate and analyse population of 136 continental strike-slip faults. Another sets cited are much smaller in number and P. A. Gillespie (see Gillespie et al., 1992) presents measurements of D_c and W_c for the set as poor as 13 thrusts.

Main investigators (e.g. Ranalli, 1977; Watterson, 1986; Walsh, Watterson, 1988; Scholz, Cowie, 1990; Cowie, Scholz, 1992; Gillespie et al., 1992) are agreed that maximum displacements, D , and maximum dimensions, W , have the systematic relationship expressed by formula

$$D = c W^n \quad (1)$$

where the value of c is determined by material properties, the most significant of which is shear modulus (Walsh, Watterson, 1988). There is no consensus among the authors regarding a value of n . In available publications proposed values of n range from 1.0 to 2.0. It so happened that two most respectable duets

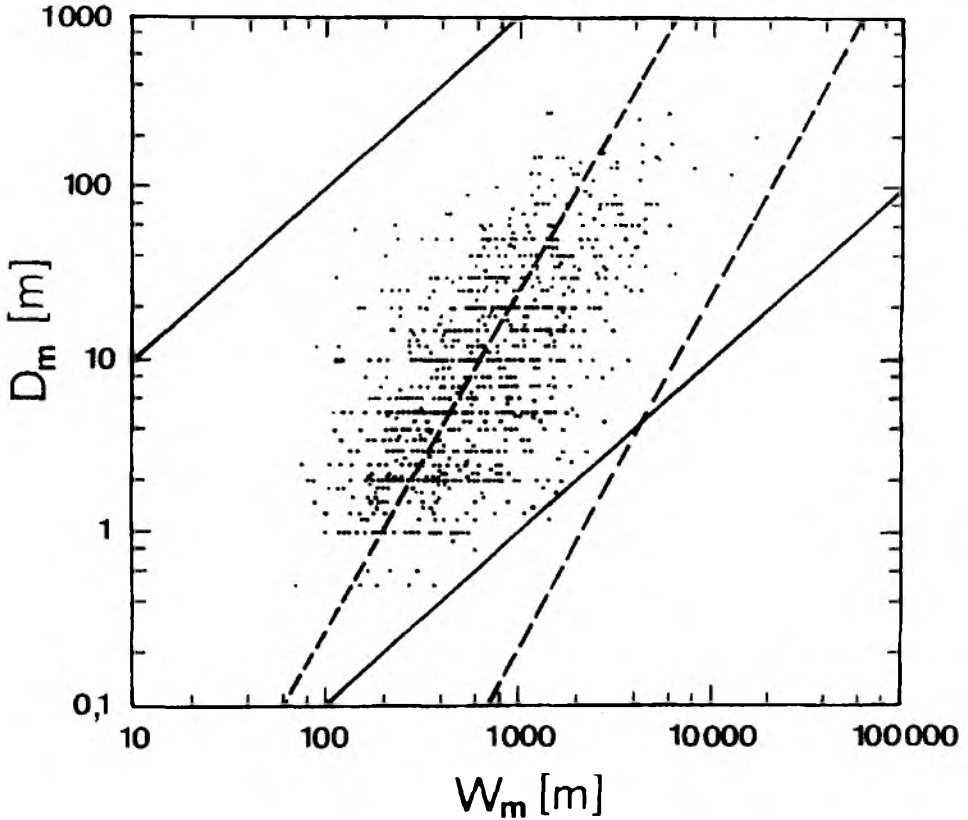


Fig. 6. Logarithmic plot of displacement, D_m , vs width, W_m , for whole dataset from northern part of the USCB

Straight lines are bounding growth curves. Broken lines with slopes of 2.0 indicate correlation proposed by J. J. Walsh & J. Watterson (1988), solid ones having slopes of 1.0 represent interpretation yielded by P. A. Cowie & C. H. Scholz (1992)

advocated extreme values of n . P. A. Cowie & C. H. Scholz from Columbia University conclude that $n = 1.0$ (e.g. Scholz, Cowie, 1990), while J. J. Walsh & J. Watterson from the Liverpool Fault Analysis Group propose value for n which is equal 2 (e.g. Watterson, 1986; Walsh, Watterson, 1988). More recently, however, the couple from Liverpool supported by co-workers (Gibson, Childs and particularly Gillespie) have changed opinion assuming a number exceeding 1.4, probably of 1.5, as the preferred value for n (Gillespie et al., 1992).

The matter in dispute, the exponent n in (1), is very important as it describes the change in fault geometry with growth. After J. Watterson (1986) a fault is assumed to grow by radial extension of the tip line with no migration of the point of maximum displacement. Displacement and dimensions are believed to be accumulated throughout the active life of a fault and this accumulation is realized by

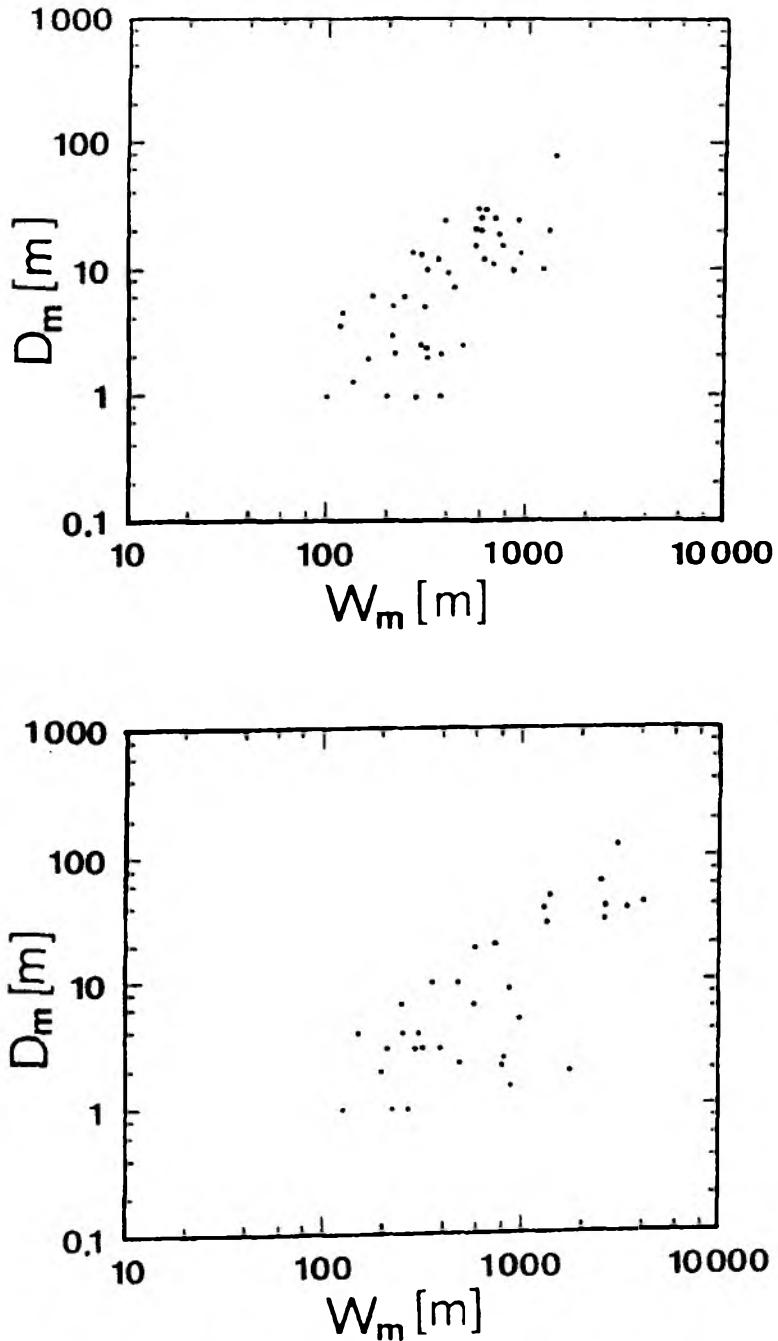


Fig. 7. Logarithmic plots of displacement, D_m , vs width, W_m , for datasets derived from some small subregions of the study area. Note that distribution is almost linear unlike the D_m against W_m distribution in the whole area (Fig. 6)

successive slips u , occurring during single seismic events. The mean slip on a fault during a single seismic cycle is directly proportional to the dimension of the surface over which the slip occurs. The u values form a series and its sum is the cumulative displacement, D , at each stage of growth. According to the models (Walsh, Watterson, 1988) stress distribution following each slip event is the same in all except scale. A fault increases in width with time and individual displacements of successive slip events must also increase. In other words, each successive slip event on the fault is larger by a constant increment than preceding one. The exponent n of 1.0 (Cowie, Scholz, 1992) would indicate no shape change, with self-similarity of form, while other values (e.g. Walsh, Watterson, 1988) describe a systematic change of shape with growth. If $n = 1.0$ the increment by which u increases in successive slip events is in linear relation to both D and W . If n exceeds 1.0 then increments of increase in u are not linearly related to either D or W . Shape of a fault grown in accordance to the models satisfies the expression (1).

In the above discussion an attention is focused on the views that are as different as possible from each other disregarding another authors' opinion. It is noteworthy that both main teams support their interpretations using the same combined datasets. The sets comprise both as small as 1m long faults with throws of several centimeters occurring in Quaternary lacustrine deposits in Japan (Muraoka, Kamata, 1983) and 100 – 1000 km long continental wrench faults with offsets exceeding 100 km (MacMillan, 1975). Decision of combining the set of minor faults from Japanese Quaternary deposits to the common analysis is controversial as the data provided by H. Muraoka & H. Kamata (1983) represent readings of lengths L , of the faults rather than the widths, W , that is contrary to other sets interpreted.

J. Watterson (1986) and J. J. Walsh & J. Watterson (1988) interpreted the data as lying on a family of lines of slope equal to 2 on log-log plot (Fig. 8). According to the model introduced by P. A. Cowie & C. H. Scholz a D/W ratio is constant for fault growing in a rock with constant shear strength (Cowie, Scholz, 1992), so in such a case data are interpreted as lying on family of lines of slope equal to 1 (Fig. 8). After all, P. A. Cowie & C. H. Scholz (1992) do declare against combining datasets together claiming that each dataset should be analysed separately because the D/W ratio is expected to vary from set to set.

Results of analysis of the USCB fault network are thought to confirm the interpretation of the Liverpool University team, especially in relation to a newest modified fault growth model (Gillespie et al., 1992) in which the increase in dimension of fault with each slip event is proportional to $W^{0.5}$. That gives rise to the value for n of 1.5. Values of n for the USCB fault set reach a range of 1.5–2.0, although D/W relationships obtained for small subareas may raise doubts. A possible explanation is that sets in small areas may be incomplete (some fault terminations lie beyond borders of the area) and therefore the n values are underestimated.

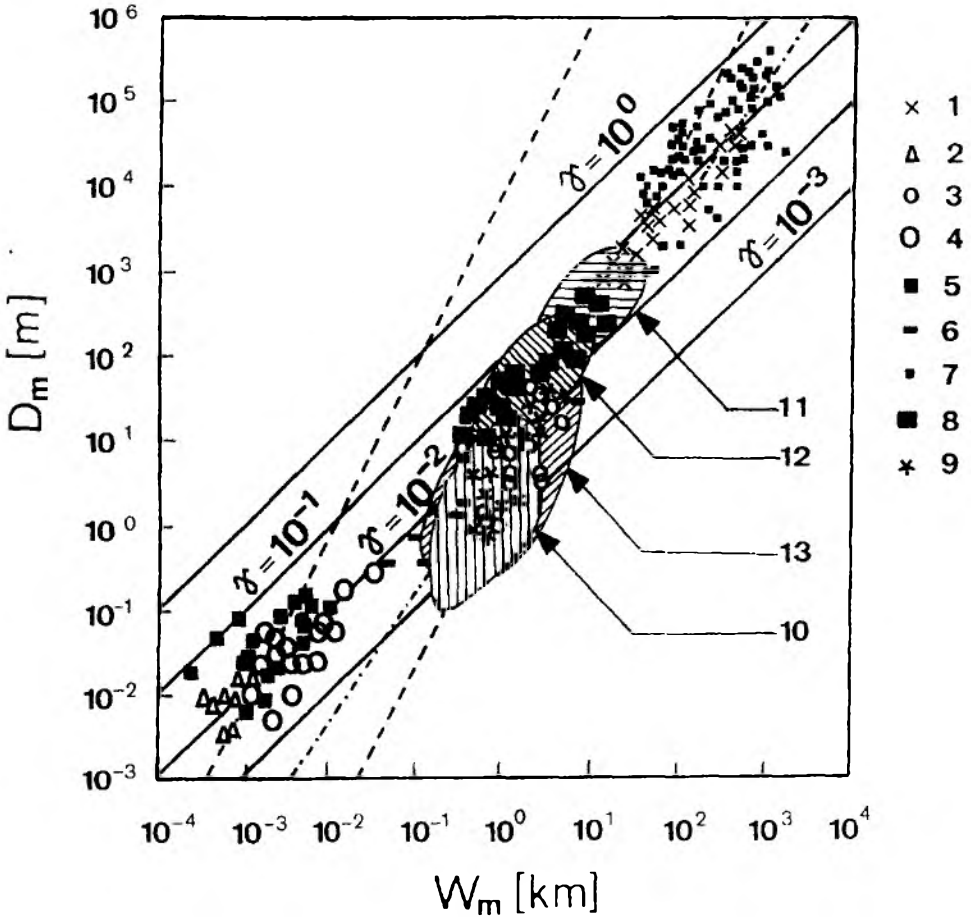
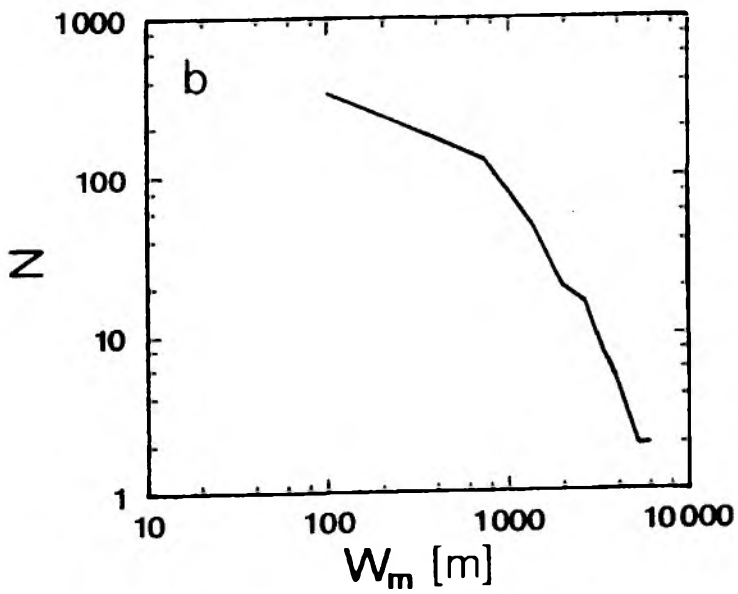
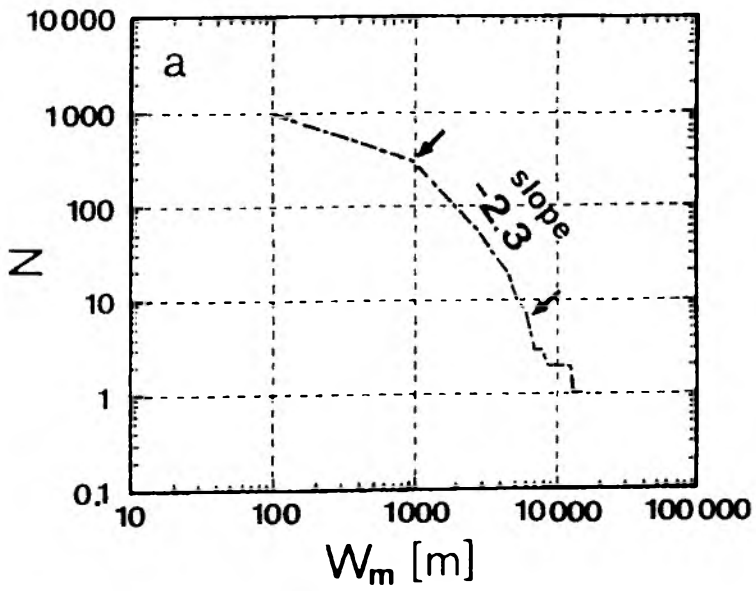


Fig. 8 Logarithmic plot of displacement, D_m , vs width W_m , for combined dataset (modified after Cowie & Scholz, 1992)

Data sets considered: 1 - Elliott (1976); 2 - Muraoka, Kamata (1983); 3 - Walsh, Watterson (1988); 4 - Peacock, Sanderson (1991); 5 - Peacock (1991); 6 - Opheim, Gudmundsson (1989); 7 - MacMillan (1975); 8 - Villemin et al (see Cowie, Scholz, 1992); 9 - Krantz (1988). Shaded elliptical fields represents additionally sets compiled by: 10 - Walsh, Watterson (1988); 11 - Marret, Allmendinger (1991); 12 - Minor Faults Research Group (1973); 13 - data set from the USCB. Dashed lines with slopes of 2.0 indicate correlation proposed by J. J. Walsh, J. Watterson (1988), solid ones having slopes of 1.0 are lines of constant ratio D_m/W_m denoted by γ values according to P. A. Cowie, C. H. Scholz (1992), dash-dot line represents regression line for the USCB data set having $n \sim 1.5$ (comparable with Gillespie et al., 1992)

It is also known that inclusion of branching splays in a dataset leads to a lower estimate of the value for n (e.g. Gillespie et al., 1992). Smaller displacement faults are usually taken to be splays off larger displacement faults, and because they terminate at intersection points where displacement is not zero, they have shorter trace lengths than isolated faults. There are fault branches occurring often in the studied part of the USCB. It is not unlikely that some of branching splays, especially those of small dimensions, were recognized as independent faults



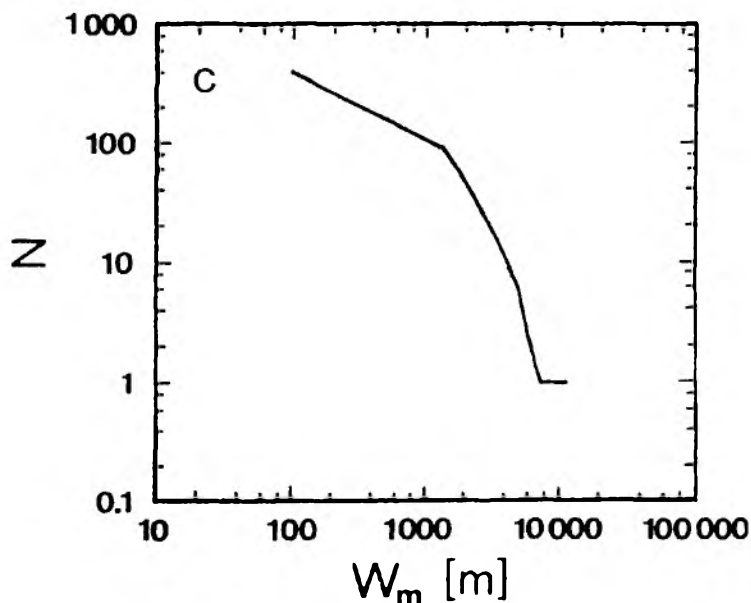


Fig. 9. Logarithmic plots of fault size distribution in northern part of the USCIB

a – for whole area, *b*, *c* – for exemplary data sets from well documented smaller regions, N – cumulative number of fault widths greater than W ; W – measured width of a fault. Right-hand segments of the frequency curves may be estimated by straight lines in both whole area and well-documented smaller regions of the Upper Silesian coalfield. Slopes of the straight segments are about -2.3 , spanning approximately 1.0 order of magnitude

(cf., Fig. 5) what might be another cause of lower than expected values of n in small size faults domain.

One can also observe, comparing the example from the U. K. with Polish one, that in the case of the USCIB constant c is lower than the c value for British coalfield. Lithological difference between the rock-complexes is a very like reason of the c values diversity.

Fault Size Frequency Distribution

Distribution of size in fault population is also the subject of analysis. Cumulative frequencies of the width W of faults are presented in respect to both whole dataset from the northern part of the USCIB and subsets distinguished for smaller areas. Populations of fault dimensions are expressed as logarithmic plots of W vs. N , where W = measured dimension and N = cumulative number of widths greater than W . The plots (Fig. 9) represent fault size populations rather than fault populations.

Shape of fault size distribution curves obtained needs a short discussion. According to D/W relationship described in the previous chapter statistical dimension of a fault with $D_m = 1$ m is not larger than 600 m. As $D_m = 1$ m is a bottom limit for dataset from the USCB there is a realistic possibility of omission of minor features even in well-documented parts of coalfield. Needless to say the omission is much bigger in unworked grounds and small size fault records are inaccurate most of all. Also in extensively worked seams faults may be missed through oversight if they not obstruct coal-winning techniques. Failure to identify a workable panel may have no technical and economic consequences for longwall mining methods applied in the USCB as far as it concerns omission of faults with D value not exceeding 2 m. These are the probable reasons of a sharp breakdowns of fault size distribution curves (Fig. 9) which occur between left-hand segments of plots representing minor features and right-hand segments, much steeper and approximately straight, which correspond with faults of larger size.

On the ground of the foregoing discussion, a conclusion was drawn that number of faults with a W value less than 1000 m is underestimated. Thus, it was decided that $W = 1000$ m is a proper bottom limit of data useful for reliable analysis of size frequency distribution in the USCB while plot of the smaller W values represents an invalid portion of curve. Similar decision concerning lower faults length cut-off is taken by C.H. Scholz & P. A. Cowie (1990) in relation to Neogene faults set in Japan. The cited authors introduce an idea that total contribution from all faults in any region can be determined from their length. Total fault moment and total fault strain only depend on the largest faults in a region. This contrasts with the idea that significant amounts of strain may be hidden in small faults below the observational limit (op. cit.).

The right-hand segments of the frequency curves may be estimated by straight lines in both whole area (Fig. 9a) and well-documented smaller regions of the Upper Silesian coalfield (Fig. 9b). The slope of the straight segments is about -2.3, spanning approximately 1.0 order of magnitude on log-log plot (Fig. 9). Small kinks in the straight segment also occur. Slope of straight lines that estimate fault size distribution reported by C.H. Scholz & P. A. Cowie (1990) is -2.1. Similarity of present results to those cited testifies the thesis that faults obey general scaling laws in their size frequency distribution. The number of faults of width $\geq W$ is (e.g. Hirata, 1989)

$$N(W) = a_1 W^{-C} \quad (2)$$

The curves are derivatives of cumulative distributions so the slopes of lines are $-(C + 1)$ so the value of C for the USCB fault size distribution is close to 1.3.

Both fault size population plots and equation of power-law distribution (2) are similar to the conventional method of representing earthquake populations

$$N(M_0) = aM_0^{-B} \quad (3)$$

where $N(M_0)$ is the number of earthquakes of seismic moment $\geq M_0$ and B has a universal value of about $2/3$.

The calculation of contemporary deformation rates from the sum of seismic moments of events provides good results. Combining scaling relations (1), (2) and (3) this method can be successfully extended to estimate strain in regions that are no longer seismically active what is demonstrated by C. H. Scholz & P. A. Cowie (1990).

Therefore the present study on faults displacement and dimension, as well as essential follow-ups are of such importance for the USCB area.

Conclusions

1. Faults in the northern part of the USCB treated as an individual set obey power-laws in both their size frequency distribution and the relationship between displacement and fault dimension. The active deep mining area of the USCB has a number of advantages for this research yielding data that are sufficiently detailed to give 3-D information on each of variables studied and providing dataset much more abundant than ones published so far. What is noteworthy the study area is not bigger than an eighth of all well-documented grounds in the coalfield.

2. Obtained results are comparable with those concerning another regions and/or groups of faults from variety of geological environments provided by other scientists. The results combined together with another datasets cover a wide range of scales. Their position in combined dataset is useful for adjusting existing models and interpretations, especially they help with stating more precisely formulae that express scaling laws governing the relationships studied.

3. The displacement/dimension relationship determined precisely implies more accurate description of fault growth over geological time. Furthermore, this relationship combined with the scaling laws ruling both the fault size frequency distribution and the size distribution of earthquakes can give a possibility to calculate total brittle strain if they are established precisely for this deformed rock-complex.

Acknowledgements

I wish to thank Christopher J. Bean in the University College Dublin for providing programs for data selection and analysis, as well as for much useful discussion.

This work is supported by Grant KBN 9 S602 045 03 from Polish Government.

References

- Cowie P. A., Scholz C. H., 1992: *Displacement – Length Scaling Relationship for Faults: Data Synthesis and Discussion*. J. Struct. Geol., **10**, 1149–1156.
- Elliott D., 1976: *The Energy Balance and Deformation Mechanisms of Thrust Sheets*. Phil. Trans. R. Soc. Lond. A., **283**, 289–312.
- Gillespie P. A., Walsh J. J., Watterson J., 1992: *Limitations of Dimension and Displacement Data from Single Faults and the Consequences for Data Analysis and Interpretation*. J. Struct. Geol., **10**, 1157–1172.
- Goszcz A., 1980: *Wpływ naprężeń tektonicznych na niektóre własności skal i warunki górnicze w północno-wschodniej części Górnośląskiego Zagłębia Węglowego*. Zesz. Nauk. AGH, **790**, Geologia, 27.
- Goszcz A., et al., 1983: *Opracowanie mapy tektonofizycznej dla Bytomskiego Zrzeszenia Kopalń Węgla Kamiennego w celu wydzielenia obszarów skłonnych do tapania*. Pol. Tow. Przyjaciół Nauk o Ziemi, Sosnowiec (unpublished).
- Hirata T., 1989: *Fractal Dimension of Fault Systems in Japan: Fractal Structure in Rock Fracture Geometry at Various Scales*. Pure Appl. Geophys., **131**, 157–170.
- Jureczka J., Kotas, A., 1995: *Upper Silesian Coal Basin*. In: *The Carboniferous System in Poland*, Eds.: A. Zdanowski, H. Zakowa, Papers of Pol. Geol. Inst., **148**, 164–173.
- Krantz R. W., 1988: *Multiple Fault Sets and Three-Dimensional Strain: Theory and Application*, J. Struct. Geol., **10**, 225–237.
- MacMillan R. A., 1975: *The Orientation and Sense of Displacement of Strike-Slip Faults in Continental Crust*. B.Sc. thesis, Carlton Univ., Ottawa (unpublished).
- Marret R., Allmendinger R. W., 1991: *Estimates of Strain due to Brittle Faulting: Sampling of Fault Populations*. J. Struct. Geol., **13**, 735–738.
- Minor Faults Research Group, 1973: *A Minor Fault System around the Otaki Area Boso Peninsula, Japan*. Earth Sci. (Chikyu Kagaku), **27**, 180–187.
- Muraoka H., Kamata H., 1983: *Displacement Distribution along Minor Fault Traces*. J. Struct. Geol., **5**, 483–495.
- Opheim J. A., Gudmundsson A., 1989: *Formation and Geometry of Fractures and Related Volcanism, of the Krafla Fissure Swarm, Northeast Iceland*. Bull. Geol. Soc. Am., **101**, 1608–1622.
- Peacock D. C. P., 1991: *Displacement and Segment Linkage in Strike-Slip Fault Zones*. J. Struct. Geol., **13**, 1025–1035.
- Peacock D. C. P., Sanderson D. J., 1991: *Displacement, Segment Linkage and Relay Ramps in Normal Fault Zones*. J. Struct. Geol., **13**, 721–733.
- Ranalli G., 1977: *Correlation between Length and Offset on Strike-Slip Faults*. Tectonophysics, **37**, 1–7.
- Rippon J. H., 1985: *Contoured Patterns of the Throw and Hade of Normal Faults in the Coal Measures (Westphalian) of Northwest Derbyshire*. Proc. Yorks. Geol. Soc., **45**, 147–161.
- Scholz C. H., Cowie P. A., 1990: *Determination of Total Strain from Faulting Using Slip Measurements*. Nature, **346**, 837–839.
- Walsh J. J., Watterson J., 1988: *Analysis of the Relationship between Displacements and Dimensions of Faults*. J. Struct. Geol., **10**, 239–247.
- Walsh J. J., Watterson J., 1990: *New Methods of Fault Projection for Coalmine Planning*. Proc. Yorks. Geol. Soc., **48**, 209–219.
- Watterson J., 1986: *Fault Dimensions, Displacements and Growth*. Pure Appl. Geophys., **124**, 365–373.